

2*p* resonance photoemission and Auger features in NiS₂ and FeS₂

S. Suga

Department of Material Physics, Graduate School of Engineering Science, Osaka University, 1-3, Machikaneyama, Toyonaka, Osaka 560-8531, Japan

A. Kimura

Department of Material Physics, Graduate School of Engineering Science, Osaka University, 1-3, Machikaneyama, Toyonaka, Osaka 560-8531, Japan
and Institute for Solid State Physics, The University of Tokyo, Minatoku, Tokyo 106-8666, Japan

T. Matsushita

Department of Material Physics, Graduate School of Engineering Science, Osaka University, 1-3, Machikaneyama, Toyonaka, Osaka 560-8531, Japan
and Japan Synchrotron Radiation Research Institute, Mikatsuki, Sayo, Hyogo 679-5198, Japan

A. Sekiyama and S. Imada

Department of Material Physics, Graduate School of Engineering Science, Osaka University, 1-3, Machikaneyama, Toyonaka, Osaka 560-8531, Japan

K. Mamiya, and A. Fujimori

Department of Physics, The University of Tokyo, Tokyo 113-0033, Japan

H. Takahashi* and N. Mori

Institute for Solid State Physics, The University of Tokyo, Minatoku, Tokyo 106-8666, Japan

(Received 21 December 1998; revised manuscript received 8 March 1999)

Resonance behaviors of the Ni and Fe 3*d*, 3*p* and 3*s* related satellite photoemission and Auger features are measured for the Ni and Fe 2*p* core excitation in NiS₂ and FeS₂. Chronological interpretation is proposed to the Ni and Fe 2*p*3*p*3*d* Auger features. A resonance satellite around the binding energy of 30 eV is identified as due to the plasmon satellite associated with the resonance-enhanced satellite of the 3*d* state.

[S0163-1829(99)05131-0]

I. INTRODUCTION

Transition-metal pyrites show interesting electronic and magnetic properties. In contrast to the metallic, ferromagnetic CoS₂ ($T_c = 120$ K), NiS₂ is an antiferromagnetic insulator ($T_N = 40$ K) and FeS₂ is a nonmagnetic insulator. The d^8 ground state in NiS₂ has the $S=1$ state, while the d^6 low-spin ground state in FeS₂ has the $S=0$ state. Photoemission spectra of these materials are repeatedly studied,¹⁻⁷ sometimes by use of synchrotron radiation and sometimes by use of x-rays. The 3*p*-3*d* resonance photoemission is utilized to reveal 3*d* satellite structures,⁵ for which the configuration-interaction cluster-model analysis has been applied.⁵⁻⁷ However, the resonance for the 3*p* core excitation is not prominent enough to discuss details of the resonance processes. The contribution of the Auger processes is rather faint. Moreover, the resonance measurement is limited in the 3*d* photoemission region.

The 2*p*-3*d* resonance is much stronger⁸ than the 3*p*-3*d* resonance. Detailed Auger features are clarified for the 2*p* core excitation not only in the 3*d* photoemission but also in the 3*p* and 3*s* photoemission regions. There is, however, a controversy on the role of the Auger contribution to the resonance.⁹ It is known that the Auger emission process

takes place when the photoexcitation energy $h\nu$ is beyond the core excitation resonance energy $h\nu_0$. The Auger electron has a smaller kinetic energy than the directly emitted photoelectron and appears in the larger binding-energy region than the direct photoelectron in the photoemission spectrum. When $h\nu$ approaches $h\nu_0$ from higher energies, the Auger structure moves closer to the direct photoemission structure. Sometimes the Auger feature overlaps completely with the direct photoemission structure for $h\nu$ very close to $h\nu_0$. Since the Auger intensity reflects the amount of core holes, it is enhanced near $h\nu_0$. If the resonance behavior of the direct photoemission at a constant E_B is solely explained by the intensity behavior of the Auger structure, one considers a simple overlap (or an incoherent superposition) of the Auger structure as an origin of the resonance behavior. It is possible, however, that the Auger process and the direct photoemission process are mixed to each other for $h\nu \sim h\nu_0$ and are no longer discriminated. Then noticeable interference takes place between the two processes and a real or coherent resonance photoemission process is observed.

The present work of 2*p*-3*d* resonance photoemission is performed to obtain more direct information on the satellites, Auger processes, and interaction energies. We report the results on NiS₂ and FeS₂ in this paper.

II. EXPERIMENT

The NiS₂ single-crystal sample was grown by the vapor transport method. The FeS₂ is a natural single crystal. The sample surface was cleaned by filing with use of a diamond file. The vacuum in the analyzer chamber was about 5×10^{-10} Torr. The photoemission measurements were performed at room temperature at the *BL-2B* undulator beam line of the Photon Factory, High Energy Accelerator Research Organization, KEK. A 10-m grazing incidence monochromator was used for the measurement. The resolution of the monochromator was set to 0.4 eV at the photon energy $h\nu = 800$ eV. The x-ray absorption (XAS) spectrum in the transition-metal (TM) *2p* core region was measured by means of the total photoelectron yield. The undulator gap was so adjusted to give the fundamental peak slightly above the $2p_{1/2}$ absorption peak. The total resolution of the photoemission measurement was set to about 0.5 eV to get reasonable statistics of the counts. All photoemission measurements were done in the wide binding energy (E_B) region from the Fermi level (E_F) to 200 eV. The energy steps of E_B were properly tuned to the smallest value in the photoemission structure regions while the spectra were crudely scanned in the structureless regions. Thus the S *2p* core photoemission was recorded in the same spectrum beside the TM *3d*, *3p*, and *3s* states and related structures. The binding energies E_B of the spectra are thus referenced to E_B of the S *2p* peak and the photoemission intensities are normalized to the intensity of the S *2p* peak.

III. RESULTS

Figures 1(a) and 1(b) show the Ni and Fe *2p* core absorption (XAS) spectra of NiS₂ and FeS₂. Besides the $2p_{3/2}$ and $2p_{1/2}$ spin-orbit split main peaks, satellite structures are recognized. The satellite structures of the XAS do not correspond directly to the conduction-band structures probed by the x-ray bremsstrahlung isochromat spectroscopy, but better correspond to the structures predicted by the configuration-interaction calculation including the full multiplet splitting.¹⁰ The alphabet shows the $h\nu$ at which the photoemission spectra in Fig. 2 are measured. The photoemission intensity is normalized in Fig. 2 as mentioned before. *a* and *b* in Fig. 2(a) correspond to the $h\nu$ that are 10 and 5 eV below *c* in Fig. 1(a). The spectra *a* to *c* in Fig. 2 are typical off-resonance spectra. The spectra *d* to *f* in Fig. 2(a) and *d* to *i* in Fig. 2(b) can be regarded as preresonance spectra. On the other hand, the spectra *l* to *o* in Fig. 2(a) and *p* and *q* in Fig. 2(b) are regarded as beyond-resonance spectra. Besides, the spectra excited near the main XAS peak are called on-resonance spectra.

Some valence-band structures in Fig. 2 are strongly enhanced as $h\nu$ approaches the peak energy of the $2p_{3/2}$ XAS $h\nu_0$ (*i* for NiS₂ and *m* for FeS₂) from the low $h\nu$ side. In Figs. 2(a) and 2(b), another prominent feature (*D4*) is clearly observed near $E_B = 30$ eV. For the resonance excitation in the $2p_{1/2}$ XAS region, one notices resonance enhancement of some parts of the valence bands as seen in *r* of Fig. 2(a). The $2p_{1/2}$ resonance is, however, not so prominent as in the case of $2p_{3/2}$ resonance and is not discussed anymore in this paper.

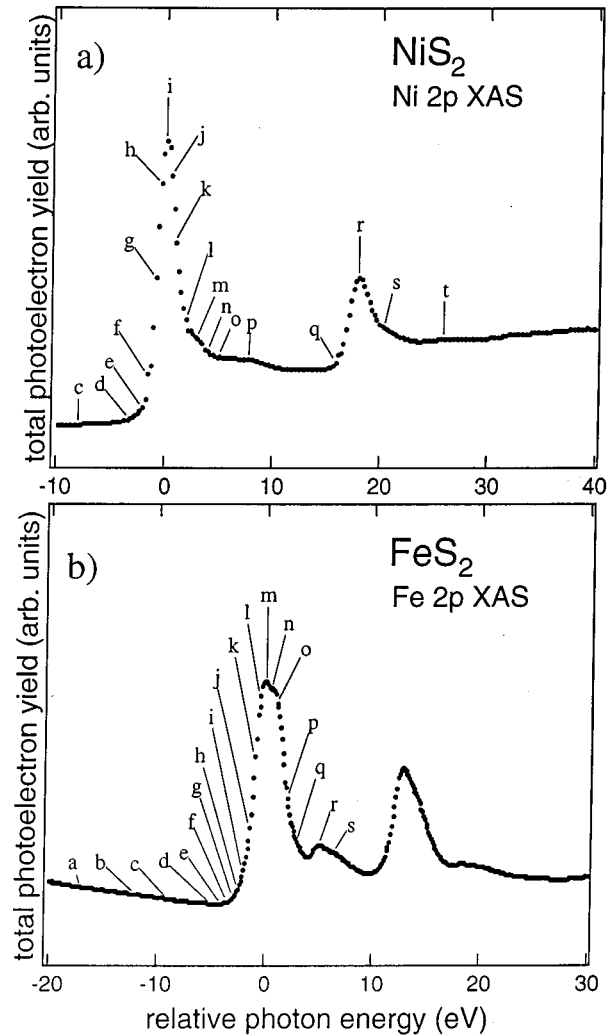
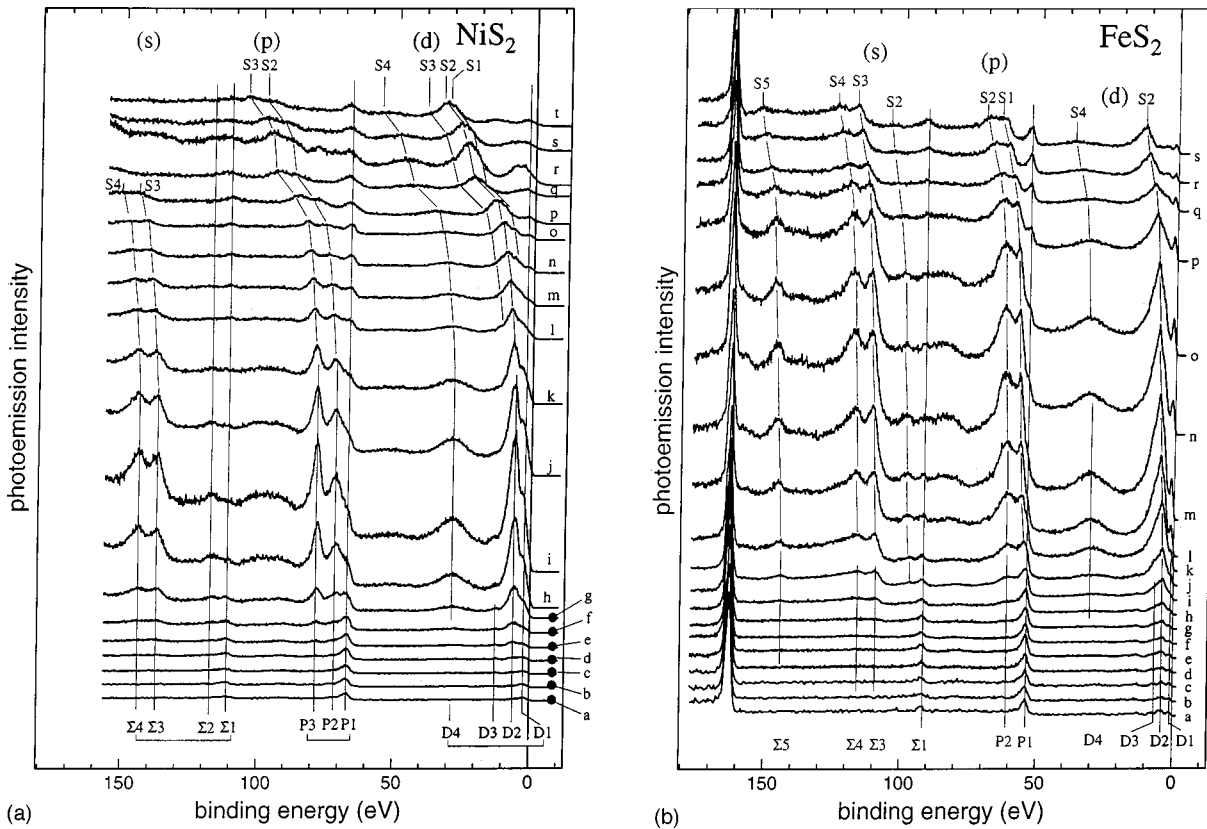


FIG. 1. Ni and Fe *2p* core absorption spectra of (a) NiS₂ and (b) FeS₂ at room temperature.

Typical preresonance spectra, *d* of NiS₂ and *h* of FeS₂, are shown in Figs. 3(a) and 3(b) compared with the on-resonance and beyond-resonance spectra in the *3p* and *3d* regions with enlarged scales. In order to clearly show structures, the relative photoemission intensity is arbitrary in Fig. 3. As seen in Fig. 3(a), the spectrum *i* of NiS₂ shows two prominent structures at 2.6 (*D1*) and 6.0 eV (*D2*) in the Ni *3d* region. In the valence-band spectrum of FeS₂, prominent enhancement is observed for the structures at 1.2 (*D1*) and 4.1 eV (*D2*) as confirmed in Fig. 2(b). In addition, one notices a stronger peak at 5.6 eV in the resonance spectrum *m*, which is clearly deviated from the energy of the structure *D2*.

In Fig. 3(a) *i*, the Ni *3p* spectra show three structures at around 67 (*P1*), 71.5 (*P2*), and 78.4 eV (*P3*). In the case of the Ni *3s* spectra, two structures are resolved near 111 ($\Sigma1$) and 118 eV ($\Sigma2$) in Fig. 2(a) *i*. Another very prominent doublet is resolved near 137 ($\Sigma3$) and 144 eV ($\Sigma4$). It is noticed that E_B of these structures remain rather constant for the $h\nu$ up to *i* from *a*. The Fe *3p* spectra in Fig. 2(b) show two structures near 54 (*P1*) and 63 eV (*P2*) for *a* to *i*. The Fe *3s* spectra show a peak $\Sigma1$ in the whole spectra from *a* to *s*. A doublet $\Sigma3$ and $\Sigma4$ as well as a structure $\Sigma5$ are resolved

FIG. 2. Photoemission spectra of (a) NiS₂ and (b) FeS₂.

for h to j . For a further increase of $h\nu$, some of the structures shift almost linearly to larger E_B with $h\nu$, reflecting the Auger character of the electron emission process. Such peaks are named S . Thus very rich and strong Auger processes are observed for the $2p$ core excitation compared to the $3p$ core excitation.⁵

The structures $D1$, $P1$, and $\Sigma1$ in NiS₂ and FeS₂ are,

however, observable at the same E_B as in the off-resonance spectra for increased $h\nu$ and are hereafter called stationary structures. In NiS₂, $S1(d)$ and $S2(d)$ converge to $D1$ and $D2$. In the case of the Ni $3p$ photoemission, however, no Auger structure converges to $P1$, whereas $S2(p)$ and $S3(p)$ converge to $P2$ and $P3$. It is impossible to recognize Auger structures continuing to $\Sigma1$ and $\Sigma2$, whereas $S3(s)$ and

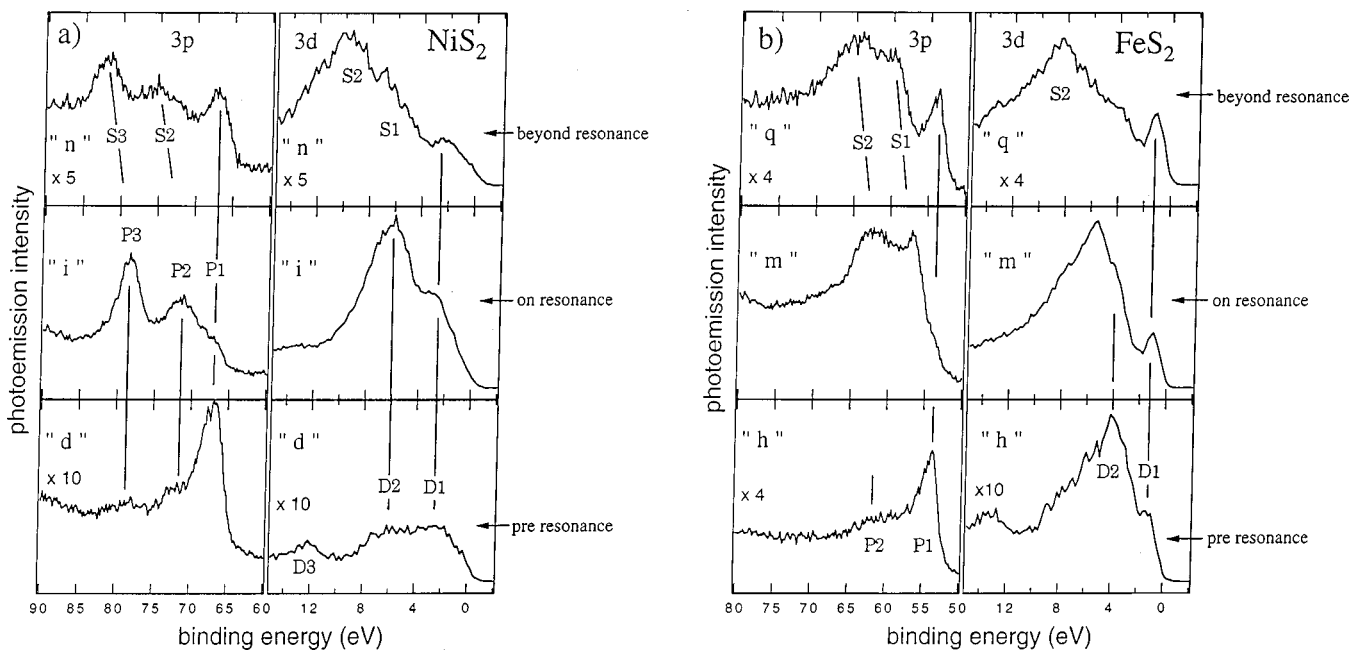


FIG. 3. Detailed photoemission spectra of (a) NiS₂ and (b) FeS₂. Typical spectra of pre-, on-, and beyond-resonance are shown with enlarged scales.

$S4(s)$ show linear shift with $h\nu$ and converge to $\Sigma 3$ and $\Sigma 4$ at $h\nu_0$ (i).

In FeS_2 , no clear Auger structure converges to $D1$, whereas $S2(d)$, $S4(d)$, $S3(s)$, $S4(s)$, and $S5(s)$ converge to $D2$, $D4$, $\Sigma 3$, $\Sigma 4$, and $\Sigma 5$, respectively. Although $S2(p)$ converges to $P2$, $S1(p)$ does not converge directly to $P1$ as shown in the on-resonance spectrum, Figs. 3(b) and 2(b) *m*, compared with *h*. Namely, the splitting energy between $S2(p)$ and $S1(p)$ is remarkably different from that between $P2$ and $P1$.

IV. DISCUSSION

Although theoretical works have been done for the resonance photoemission under the $2p$ core excitation without explicitly taking into account the Auger process,¹⁰ consideration of the Auger process is quite important for an intuitive interpretation of the experimental results. First, we discuss the photoemission features in the Ni $3p$ core region. $S2(p)$ and $S3(p)$ are interpreted as the Ni $2p3p3d$ ($L_3M_{2,3}M_{4,5}$) Coster-Kronig Auger processes from their energy positions.

This doublet structure is very prominent for the excitations from *h* to *m* in Fig. 2(a). If the majority of $3d$ spin is assumed to be the up (\uparrow) spin in the d^8 ground state of Ni in NiS_2 , the $2p$ resonance excitation takes place from the $2p(\downarrow)$ core state to the empty $3d(\downarrow)e_g$ state. By taking the quantization axis as the z axis, we consider the exchange splitting to be proportional to the product of $S_z(3d)$ and $S_z(3p)$ of the final states. Then the above $2p3p3d$ Auger transition has the following two possibilities (cases 1 and 2).

Case (1). $2p(\downarrow)3p(\downarrow)3d(\uparrow)$ with $S_z(3d)=0$ or $2p(\downarrow)3p(\downarrow)3d(\downarrow)$ with $S_z(3d)=+1$. In this case, the $3p(\downarrow)$ electron fills the empty $2p(\downarrow)$ state with the resultant $3p$ spin of $S_z(3p)=+1/2$. Either \uparrow or \downarrow $3d$ electron is excited and the resultant total spin of the $3d$ electrons can be 0 or +1.

Case (2). $2p(\downarrow)3d(\downarrow)3p(\downarrow)$ with $S_z(3p)=+1/2$ or $2p(\downarrow)3d(\downarrow)3p(\uparrow)$ with $S_z(3p)=-1/2$. In this case, the $3d(\downarrow)$ electron fills the empty $2p(\downarrow)$ state and either the \downarrow or \uparrow $3p$ electron is ejected. Then the total spin of the $3d$ electrons is $S_z(3d)=+1$ and the total spin of the $3p^5$ electrons can be $S_z(3p)=\pm\frac{1}{2}$.

By representing the spin-exchange interaction between the $S_z(3d)$ and $S_z(3p)$ spins by $J(d,p)$, the above two cases (1) and (2) are thought to provide a doublet with different energy splittings. Namely, the splittings are approximately (1) $J(d,p)/2$ and (2) $J(d,p)$, respectively.

In the case of the FeS_2 with a fully occupied t_{2g} state, corresponding doublet Auger features are observed in Figs. 2(b) as $S1(p)$ and $S2(p)$. For the excitation within the Fe $2p_{3/2}$ main absorption band, the probabilities of creating holes in the $2p(\uparrow)$ or $2p(\downarrow)$ states are just equal in FeS_2 . If the decay of case (2) takes place, $S_z(3d)=0$ and no exchange splitting is expected. In case (1) with $2p(\uparrow)$ or $2p(\downarrow)$, $S_z(3p)$ becomes $-1/2$ or $+1/2$. For the $2p(\uparrow)$, $S_z(3d)$ can be 0 or +1, while $S_z(3d)$ can be 0 or -1 for the $2p(\downarrow)$. Then the Auger features will give a doublet split by $1/2J(d,p)$ for either $2p(\uparrow)$ or $2p(\downarrow)$ excitation. The observation of the clear doublet Auger features shows that case (1) is dominant in the $2p3p3d$ Auger decay in FeS_2 . Since the symmetries of the core hole ($2p$) and the relaxing electron

($3p$) are the same (both are p like), case (1) may be much favored over case (2). The corresponding doublet splitting of the $2p3p3d$ Auger features in NiS_2 is interpreted in the same manner. In this way, a chronological interpretation of the $2p3p3d$ Auger process is proposed. In other words, it is experimentally confirmed that the $2p3d3p$ Auger process is much weaker than the $2p3p3d$ Auger process. Here one notices for FeS_2 that the $S1(p)$ is much sharper than $S2(p)$ in the resonance Auger spectra in *m* and *l* in Fig. 2(b). The $S1(p)$ corresponds to the Auger emission with $S_z(3d)=0$ in the final state, whereas the $S2(p)$ corresponds to $S_z(3d)=\pm 1$. $S_z(3d)=0$ may be the reason why the $S1(p)$ has a rather narrow width due to the absence of the exchange interaction. In the case of NiS_2 , the $S2(p)$ corresponds to $S_z(3d)=+1$ and $S3(p)$ corresponds to $S_z(3d)=0$. The slightly narrower width of $S3(p)$ in NiS_2 may be reflecting this situation.

Under the preresonance condition, three structures are recognized in NiS_2 as $P1$, $P2$, and $P3$ in Figs. 3(a) *d*. The splitting between $P2$ and $P3$ (7 eV) is comparable to that between $S2(p)$ and $S3(p)$, suggesting a similar origin of the doublet. Here the results of metallic Ni are reviewed for comparison. In the photoemission spectrum of metallic Ni calculated by the cluster model,^{11,12} the similar triplet structures ($P1'$, $P2'$, and $P3'$) are recognized and interpreted as $3p^5 3d^{10} + 3p^5 3d^9$ (${}^3F+{}^1D$) corresponding to $P1'$, $3p^5 3d^9$ (${}^3P+{}^3D$) to $P2'$, and $3p^5 3d^9$ (${}^1F+{}^1P$) to $P3'$. The interpretation for Ni metal $3p$ photoemission is confirmed by our spin-polarized photoemission experiment on core levels.¹³ The splitting between the $P2'$ and $P3'$ is mostly ascribed to the spin exchange splitting. Since the $3p^5 3d^{10}$ state is predominating in the $P1'$ structure, the splitting between the $P1'$ and ($P2'$, $P3'$) is mostly attributed to the splitting by the charge-transfer mechanism. The interpretation of $P1$, $P2$, and $P3$ in NiS_2 is very analogous to the case of Ni. The charge-transfer hybridization may be slightly modifying the splitting patterns of the stationary structures ($P1$, $P2$, and $P3$).

In the $3p$ spectra of FeS_2 , one can only see a doublet $P1$ and $P2$ for the preresonance excitation as shown in Fig. 3(b) *h*. The splitting of the doublet $P1$ and $P2$ of about 7.8 eV is appreciably larger than the exchange splitting of the doublet Fe $2p3p3d$ Auger features $S1$ and $S2$ of 4.8 eV in FeS_2 . This result clarifies the different mechanisms for the doublet. The doublet observed under the preresonance excitation is due to the charge transfer splitting ($p^5 d^7 L$ for the main peak and $p^5 d^6$ for the satellite where L stands for the ligand hole), whereas the doublet Auger features $S1(p)$ and $S2(p)$ are due to the p - d exchange interaction. The absence of the exchange splitting in the preresonance spectra is consistent with the low-spin d^6 configuration [with $S_z(3d)=0$] in the ground state.

Now we discuss the Ni $3s$ structures $\Sigma 1$ and $\Sigma 2$. The relative intensity changes considerably with $h\nu$ in consistency with a theoretical prediction.¹⁰ These structures may be resulting from the mixed effects of both the charge transfer and exchange splitting.¹⁰⁻¹³ For FeS_2 a single stationary structure $\Sigma 1$ is observed in the off- and preresonance conditions. The absence of the $3s$ - $3d$ exchange interaction due to the $S_z(3d)=0$ is responsible for the line shape. The weak Auger feature $S2(s)$ observed in the on- and beyond-

resonance conditions may be ascribed to the $2p3s3d$ Auger decay.

One also notices prominent doublet Auger features $S3(s)$ and $S4(s)$ in both NiS_2 and FeS_2 . Very similar features are also observed for CoS_2 . These results suggest that the origin of the doublet is not related to the $3d$ states. The energy positions suggest an interpretation as the $3p^4$ states. Then the energy splitting is ascribed to the p - p exchange interaction. The splitting of this doublet $S3$ and $S4$ is of about 7 eV. Under the on- and preresonance conditions, structures $\Sigma3$ and $\Sigma4$ are observed. The energy splitting is equal to the $S3$ - $S4$ splitting. The $3s^23p^43d^{n+1}$ states ($\Sigma3$ and $\Sigma4$) strongly couple with the $3s^13p^63d^n$ states ($\Sigma1$ and $\Sigma2$ states in NiS_2 and $\Sigma1$ state in FeS_2) by the intraatomic configuration interaction, where n is the number of the d electrons in the ground state. Then finite intensity is given to the $3s^23p^43d^{n+1}$ states. When the Auger features $S3(s)$ and $S4(s)$ approach the structures $\Sigma3$ and $\Sigma4$, the latter structures are resonantly enhanced. Their intensities are, however, not linear to the absorption intensity (or number of the $2p$ core holes) as seen from the comparison of i and h in Fig. 2(a) or k , l , and m in Fig. 2(b). This result supports the coherent resonance enhancement mechanism of the configuration interaction satellite rather than a simple incoherent overlap of the Auger features. The Auger feature $S5$ in FeS_2 is interpreted as the $2p3p3s$ decay.

As for the $P3$ and $P2$ structures in NiS_2 , their intensities are not linear to the core absorption intensity shown in Fig. 1(a) and the line shapes in g - j are much different from the beyond-resonance Auger spectra, for example, o . The behavior of the structure $P1$ is neither explained by the incoherent superposition of the Auger emission structures. The intensity behavior of the $D2$ and $D1$ is also not explained by considering the simple incoherent overlap of the Auger structures $S3(d)$, $S2(d)$, and $S1(d)$. We conclude that the resonance behaviors of the structures $D1$, $D2$, $P1$, $P2$, and $P3$ are due to coherent resonance photoemission processes.

In the case of FeS_2 , the line shapes of the Auger features $S2(p)$ and $S1(p)$ noticeably change when they approach the structures $P2$ and $P1$. Their intensities are not linear to the core absorption intensity, suggesting the interference with the direct photoemission processes. As for the $3d$ photoemission, no Auger feature overlaps with the structure $D1$. Still the resonance enhancement is clearly observed for $D1$. The intensity of this peak as a function of $h\nu$ has shown a Fano-type shape with a dip on the lower $h\nu$ side. Thus the resonance behaviors of $D1$, $P1$, and $P2$ are ascribed to coherent resonance photoemission processes.

In NiS_2 , the structure $D1$ is interpreted as the d^8L final states and the structure $D2$ is ascribed to the d^7 final states in the configuration-interaction theory.⁵ The structure $D3$ may be ascribed to the $S 3s$ state. In FeS_2 , the configuration-interaction calculation has not yet been done. In the band model, the $D1$ is ascribed to the fully occupied t_{2g} band and the structures $D2$ and $D3$ are interpreted as the $S 3p$ band hybridized with the $\text{Fe } 3d e_g$ states.

In the $3d$ photoemission region, we have also noticed a remarkable satellite $D4$ appearing around $E_B = 30$ eV for the $2p_{3/2}$ core excitation. When we excite a higher $h\nu$ absorption

tail, the E_B of this structure moves linearly with $h\nu$ as represented by the structure $S4(d)$. The resonance behavior of the structure $D4$ and the energy shift of the structure $S4(d)$ are observed through NiS_2 , CoS_2 , and FeS_2 . To our knowledge, however, there has been no interpretation for this state.

We may first consider the possibility of the Auger process. When the TM $2p$ electron is excited to the continuum state for $h\nu > h\nu_0$, the TM $3d$ electron may fill the empty TM $2p$ core hole state. Since the TM $3d$ state is strongly hybridized with the $S 3p$ and $3s$ states,^{5,14} this also induces the sudden change of the Coulomb potential on the S site. Then either the $S 3s$ or $S 3p$ electron can be ejected as an Auger electron. If the $S4(d)$ is interpreted as the TM $2pS3sS3p$ Auger transition, the effective correlation energy $U_{\text{eff}}(3s,3p)$ between the $S 3s$ and $S 3p$ holes is evaluated as 12 eV by assuming the E_B of the $S (3s)$ state as 13 eV and that of the $S (3p)$ state as 5 eV in NiS_2 . The $S 3s$ state has two components due to the molecular-orbital formation in the S_2 molecule, which nearly octahedrally surrounds the Ni atom. The E_B of these $S 3s$ states ranges from 14 to 15 eV according to the molecular-orbital studies.¹ XPS studies have revealed that the $S 3s$ states in NiS_2 are at $E_B = 12.5$ and 17 eV (Ref. 2) or 12.9 and 16.6 eV.³ Even when we take $E_B(S 3s) = 17$ eV, the $U_{\text{eff}}(3s,3p)$ becomes 8 eV in the above model, which is still unusually large. If we interpret the structure as two $3s$ holes are left behind the Ni $2p$ core hole Auger decay, the $U_{\text{eff}}(3s,3s)$ can be smaller. However, we have not seen the possible TM $2pS3pS3p$ Auger features in the smaller E_B region. So we should consider another possibility for the structure $D4$.

One may think that the structure $D4$ is a plasmon satellite. The plasmon energy is estimated as 21 eV (23 eV) for NiS_2 (FeS_2) from optical spectra.⁴ It is noticed that the $D4$ - $D2$ splitting is roughly 22 eV in NiS_2 and 26 eV in FeS_2 . Considering the broad spectral shape of the structure $D4$, these energies rather correspond to the reported bulk-plasmon energies. One may also remember the unidentified structures in the Ni and Fe $3p$ core regions. Namely, one observes broad structures in $E_B = 88$ -108 eV in NiS_2 and in $E_B = 78$ -90 eV in FeS_2 . The energy splitting of these structures from the strong $3p$ photoemission satellite structures is of a comparable amount as the bulk-plasmon energy.

Plasmon satellites associated with Auger peaks are sometimes reported.¹⁵ The resonance satellite of the $3d$ and $3p$ photoemission under the $2p$ core resonance excitation is attributed to the coherent interference between the direct photoemission and the direct recombination-type Auger decay following the core absorption. Therefore we interpret the structure $D4$ and $S4$ as well as the corresponding structure in the $3p$ core region as the bulk-plasmon satellite associated with the $3d$ and $3p$ resonance satellite and the corresponding Auger structure. This interpretation is more plausible than the interatomic Auger decay model, which fails to explain the above-mentioned broad features in the $3p$ core region. Finally the $S1(d)$ and $S2(d)$ in NiS_2 are ascribed to the Ni $2p3d3d$ Auger transition. When $S2(d)$ approaches, the $D2$ is strongly enhanced reflecting its d^7 character. In FeS_2 , the $S2(d)$ is the Fe $2p3d3d$ Auger transition.

V. CONCLUSION

In conclusion, we have studied the $2p$ core resonance photoemission behavior of NiS_2 and FeS_2 . Various satellites

and Auger structures are resolved. Coherent interference behaviors of the resonance photoemission processes are experimentally clarified. Chronological interpretation is presented for the TM $2p3p3d$ Auger features. Plasmon satellites associated with the $3d$ and $3p$ resonance satellites and Auger emission are identified. It is found that various spectral features in low-spin FeS_2 are a result of the $S_z(3d)=0$ character of the $3d$ electrons in the ground state. For example, the $3s$ photoemission shows a single structure not split by the exchange interaction. The doublet features $P1$ and $P2$ in FeS_2 in contrast to the triplet features $P1$, $P2$, and $P3$ in NiS_2 are also due to the absence of the p - d exchange interaction. The sharp spectral feature of the $S1(p)$ resonance Auger structure in FeS_2 in contrast to the broader $S2(p)$ Auger structure is interpreted by considering the $S_z(3d)=0$ character in the corresponding final state. The $2p3p3d$ Auger emission has shown a doublet in FeS_2 , because the

$S_z(3d)$ in the final state can be either 0 or ± 1 and the Auger emission is split by the p - d exchange interaction. The comparable splitting in NiS_2 is interpreted in the same manner since $S_z(3d)$ in the final state is either 0 or $+1$.

Without detailed theoretical calculations, one can thus reveal some details of the resonance photoemission processes by high resolution resonance photoemission spectroscopy in a wide energy region.

ACKNOWLEDGMENTS

The authors acknowledge Dr. A. Tanaka and Professor T. Jo for stimulating discussions. This work was supported by the Grant-in-Aid for COE Research (Grant No. 10CE2004) of the Ministry of Education, Science, Sports and Culture, Japan. The experiments were performed under the approval of the PF Program Advisory Committee.

*Present address: College of Humanities and Sciences, Nihon University, Setagaya-ku, Tokyo 156, Japan.

¹E. K. Li, K. H. Johnson, D. E. Eastman, and J. L. Freeouf, *Phys. Rev. Lett.* **32**, 470 (1974).

²A. Ohsawa, H. Yamamoto, and H. Watanabe, *J. Phys. Soc. Jpn.* **37**, 568 (1974).

³H. van der Heide, R. Hemmel, C. F. van Brugger, and C. Haas, *J. Solid State Chem.* **33**, 17 (1980).

⁴S. Suga, K. Inoue, M. Taniguchi, S. Shin, M. Seki, K. Sato, and T. Teranishi, *J. Phys. Soc. Jpn.* **52**, 1848 (1983).

⁵A. Fujimori, K. Mamiya, T. Mizokawa, T. Miyadai, T. Sekiguchi, H. Takahashi, N. Mori, and S. Suga, *Phys. Rev. B* **54**, 16 329 (1996).

⁶K. Mamiya, T. Mizokawa, A. Fujimori, T. Miyadai, N. Chandrasekharan, S. R. Krishnakumar, D. D. Sarma, H. Takahashi, N. Mori, and S. Suga, *Phys. Rev. B* **58**, 9611 (1998).

⁷A. E. Bocquet, K. Mamiya, T. Mizokawa, A. Fujimori, T. Miyadai, H. Takahashi, N. Mori, and S. Suga, *J. Phys.: Condens.*

Matter **8**, 2389 (1996).

⁸L. H. Tjeng, C. T. Chen, J. Ghijsen, P. Rudolph, and F. Sette, *Phys. Rev. Lett.* **67**, 501 (1991).

⁹M. F. Lopetz, A. Hoehr, C. Laubschat, M. Domke, and G. Kaindl, *Europhys. Lett.* **20**, 357 (1992).

¹⁰A. Tanaka and T. Jo, *J. Phys. Soc. Jpn.* **63**, 2788 (1994).

¹¹G. van der Laan, M. Surman, M. A. Hoyland, C. F. J. Flipse, B. T. Thole, Y. Seino, H. Ogasawara, and A. Kotani, *Phys. Rev. B* **46**, 9336 (1992), and references therein.

¹²A. Tanaka and T. Jo, *J. Phys. Soc. Jpn.* **64**, 4013 (1995), and references therein.

¹³Y. Saitoh, T. Matsushita, S. Imada, H. Daimon, S. Suga, J. Fujii, K. Shimada, A. Kakizaki, K. Ono, M. Fujisawa, T. Kinoshita, and T. Ishii, *Phys. Rev. B* **52**, R11 549 (1995).

¹⁴A. Fujimori, K. Terakura, M. Taniguchi, S. Ogawa, S. Suga, M. Matoba, and S. Anzai, *Phys. Rev. B* **37**, 3109 (1988).

¹⁵O. Gunnarsson, K. Schönhammer, J. C. Fuggle, and R. Lasser, *Phys. Rev. B* **23**, 4350 (1981).